Am J Cancer Res 2025;15(7):2988-3002
www.ajcr.us /ISSN:2156-6976/ajcr0165304

Original Article

La-related protein 1 drives malignant progression and epithelial-mesenchymal transition in anaplastic thyroid carcinoma

Changtian Yin[1,2,3*], Jinpeng Wen[1,4*], Zhekuan Lv[4], Lingling Ding[1], Mojiao Lu[4], Yawen Guo[1,2,3], Lingli Jin[1,6], Xiabin Lan[5], Qingliang Wen[5#], Chuanming Zheng[1,2,3#]

[1]Otolaryngology, Head and Neck Center, Cancer Center, Department of Head and Neck Surgery, Zhejiang Provincial People's Hospital (Affiliated People's Hospital), Hangzhou Medical College, Hangzhou 310014, Zhejiang, China; [2]Zhejiang Provincial Clinical Research Center for Head and Neck Cancer, Hangzhou 310014, Zhejiang, China; [3]Zhejiang Key Laboratory of Precision Medicine Research on Head and Neck Cancer, Hangzhou 310014, Zhejiang, China; [4]Postgraduate Training Base Alliance of Wenzhou Medical University (Zhejiang Provincial People's Hospital), Wenzhou 325000, Zhejiang, China; [5]Zhejiang Cancer Hospital, Hangzhou Institute of Medicine (HIM), Chinese Academy of Sciences, Hangzhou 310022, Zhejiang, China; [6]Tongji University School of Medicine, No. 500 Zhennan Road, Shanghai 200331, China. [*]Equal contributors. [#]Co-corresponding authors.

Received April 13, 2025; Accepted June 24, 2025; Epub July 15, 2025; Published July 30, 2025

Abstract: Anaplastic thyroid cancer (ATC) is an extremely aggressive and lethal malignancy characterized by a very short average survival time following diagnosis. Understanding the molecular mechanisms that drive this aggressiveness is vital for developing effective therapies. This study aimed to elucidate the role and function of La-related protein 1 (LARP1) in ATC progression. We quantitatively analyzed LARP1 expression in patient samples and ATC cell lines. Functional assays were performed to investigate LARP1's involvement in cancer-related processes, including inhibition of apoptosis, promotion of cell cycle progression, proliferation, colony formation, migration, and invasion. Our results revealed significantly elevated LARP1 expression in ATC tissues, which may be associated with poor patient prognosis. Experimental data demonstrated that LARP1 enhances oncogenic activities, promoting proliferative and invasive behaviors. These findings provide compelling evidence that LARP1 plays a crucial role in ATC malignancy, offering insights into pathophysiology and potential therapeutic targets.

Keywords: Anaplastic thyroid cancer, LARP1, malignancy, therapeutic target

Introduction

Thyroid cancer is the most prevalent endocrine malignancy, with anaplastic thyroid carcinoma (ATC) accounting for only 1%-2% of cases but responsible for approximately 50% of thyroid cancer-related deaths [1, 2]. ATC is a poorly differentiated tumor and is considered the deadliest human cancer worldwide, notable for its rapid progression and lethality [3]. Median overall survival is approximately 3-5 months post-diagnosis, with near 100% disease-specific mortality [4, 5]. Currently, the precise pathogenesis of ATC remains unclear, and effective treatments to extend survival are limited [6, 7]. Conventional therapies such as chemotherapy, radioiodine ablation, and radiotherapy provide minimal benefit [8], with over 40% of patients presenting with distant metastases at diagnosis. Death is frequently due to asphyxia caused by local tumor growth and metastasis [9, 10]. These challenges highlight the urgent need for novel therapeutic strategies and deeper understanding of molecular drivers in ATC.

RNA-binding proteins are essential regulators of cell pluripotency and self-renewal, and their dysregulation is implicated in various diseases including cancer [11, 12]. La-related protein 1 (LARP1), a member of the conserved LARP family, contains a La domain critical for RNA binding [13, 14]. Predominantly cytoplasmic, LARP1 regulates mRNA translation and stability, influencing protein synthesis, apoptosis, prolifera-

https://doi.org/10.62347/GUPU2399

tion, and migration [15]. Elevated LARP1 expression correlates with poor prognosis in multiple cancers such as liver, ovarian, lung, and colorectal cancers, associating with tumor size, survival, and clinical features [13, 16-19]. Notably, LARP1 mRNA is significantly upregulated in hepatocellular carcinoma, correlating with adverse outcomes [18]. In ovarian cancer patients, circulating levels of LARP1 correlate with tumor load, and LARP1 acts as a post-transcriptional facilitator of apoptosis evasion in ovarian cancer cells [13]. High LARP1 protein levels also associate with progression and poor survival in non-small cell lung and cervical cancers [17]. However, the expression of LARP1 in ATC and its specific functions and mechanisms of action remain unexplored. Understanding LARP1 in ATC may reveal novel molecular mechanisms and therapeutic targets. The aim of this study was to investigate the expression of LARP1 in ATC and to elucidate its function, thereby offering new perspectives for targeted therapeutic strategies in ATC.

Material and methods

Source of specimens

We retrospectively analyzed pathological specimens collected at Zhejiang Cancer Hospital from patients who underwent surgery in the Department of Head and Neck Surgery between January 1, 2016, and December 31, 2017. The study included 10 pairs of primary papillary thyroid carcinoma (PTC) samples and their adjacent normal thyroid tissues, along with 6 anaplastic thyroid carcinoma (ATC) samples. Data access occurred on December 12, 2022, following approval by the Medical Ethics Committee of Zhejiang Cancer Hospital (approval number: IRB-2022-741). Written informed consent was obtained from all patients prior to their participation in the study. The study complied fully with the Declaration of Helsinki, ensuring patient rights and confidentiality. Samples were selected based on routine pathological diagnoses confirmed by histopathological examination and staged postoperatively according to the 8th edition of the TNM system by UICC/AJCC [6]. PTC diagnosis was based on characteristic nuclear features, including enlargement, overlapping, grooves, and Orphan Annie eye nuclei. For ATC, the diagnosis was based on the presence of undifferentiated, pleomorphic tumor cells lacking conventional thyroid cancer histological features. Additionally, immunohistochemical staining was utilized to support the diagnostic process. Clinicopathological information for these patients was collected, and LARP1 protein expression and intensity were evaluated immunohistochemically by hospital pathologists.

Immunohistochemistry and histology

Cancerous and adjacent non-cancerous tissues from PTC and ATC patients at Zhejiang Cancer Hospital were collected. ATC tumor tissues were fixed in formalin, processed, and embedded in paraffin. Sections of 5 μm thickness were mounted on positively charged slides. Immunohistochemical staining was performed using standard protocols, with overnight incubation at 4°C using primary antibodies against LARP1 diluted 1:200. Detection employed conjugated secondary antibodies (1:200) and diaminobenzidine (DAB) chromogen. Pathologists quantified LARP1 staining in five representative fields per sample. Expression scoring was defined as follows: 0-5% (-), 5-25% (1+), 25-50% (2+), 5-75% (3+), and 75-100% (4+). Scores of 3+ and 4+ were considered high expression, while -, 1+, and 2+ were considered low.

Cell lines and cell culture

The human normal thyroid cell line NTHY-3, PTC cell lines TPC-1 and IHH4, as well as ATC cell lines 8505C, KHM-5M, CAL-62, C643, and BTH101 were all obtained from the National Infrastructure of Cell Line Resource in Shanghai, China. Except for BTH101 cells, which were cultured in DMEM supplemented with 10% fetal bovine serum (FBS), all other cell lines were maintained in RPMI-1640 medium (Invitrogen, Carlsbad, CA, USA) supplemented with 10% FBS. All cells were incubated at 37°C in a humidified atmosphere containing 5% CO_2. Initial screening of LARP1 protein expression across five ATC cell lines (CAL-62, KHM-5M, 8505C, C643, and BTH101) revealed that CAL-62 and KHM-5M exhibited the highest levels (**Figure 1C**), making them optimal models for functional loss-of-function studies. Therefore, subsequent experiments were conducted using these two cell lines.

Cell transfection

To explore the role of LARP1 in ATC, three siRNA sequences targeting LARP1 and corresponding

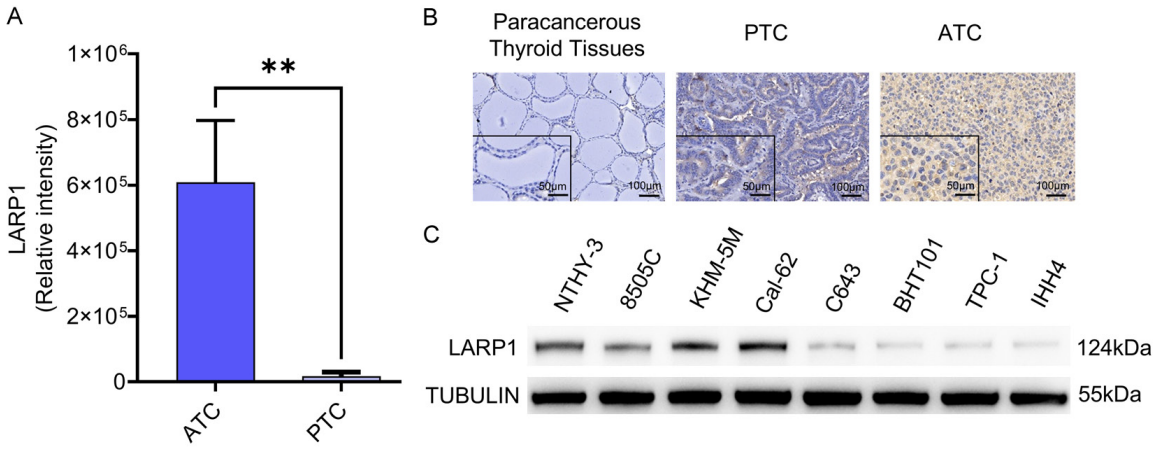

Figure 1. LARP1 is highly expressed in anaplastic thyroid carcinoma. A. Proteomic analysis to determine the relative expression levels of LARP1 in PTC (n = 6) compared to ATC (n = 6), $^{**}P < 0.01$, compared with PTC. B. Immunohistochemical staining of thyroid specimens. Comparison of LARP1 levels in tissues of peritumoral thyroid tissues, PTC and ATC, Bar = 100 μm; in the lower left inset, Bar = 50 μm; images were taken at 20× magnification. C. Detection of LARP1 gene expression in PTC (IHH4, TPC-1) and ATC (8505C, CAL-62, KHM-5M, C643, BHT101) cells using Western blot.

Table 1. SiRNA sequences of LARP1

Gene name	Target sequence
Si-LARP1-1	Sense-1: GGUGACUUUGGAGAUGCAAdTdT
	Anti-sense-1: UUGCAUCUCCAAAGUCACCdTdT
Si-LARP1-2	Sense-2: GAUAGUAAGGAGAGUCCAAdTdT
	Anti-sense-2: UUGGACUCUCCUUACUAUCdTdT
Si-LARP1-3	Sense-3: GAUGAGACAUCGAGUGUGAdTdT
	Anti-sense-3: UCACACUCGAUGUCUCAUCdTdT

Table 2. Primer sequences used for RT-qPCR

Gene name	Primer sequences
LARP1	Forward: 5'-ACACAAGTGGGTTCCATTACAAA-3'
	Reverse: 5'-CTCCGCGATTGGCAGGTAT-3'
18s-rRNA-hu-R	Forward: 5'-GGTCGGAGTCAACGGATTTG-3'
	Reverse: 5'-ATGAGCCCCAGCCTTCTCCAT-3'

negative controls (NC) were obtained from Beijing Tsingke Biotech Co., Ltd. (**Table 1**). CAL-62 and KHM-5M cells in the exponential growth stage were distributed into six-well plates with 120,000 cells per well. Cells were transfected with Lipofectamine® 3000 reagent (Invitrogen, Grand Island, NY, USA) in Opti-MEM® I (GIBCO/BRL) when reaching a confluence level between 40% and 60%. Following a 12-hour incubation period at 37°C in an environment with 5% CO_2, the old medium was swapped out for a new complete culture medium. After an additional 48 hours of incubation, the cells were harvested for further cellular function assays.

Quantitative real-time polymerase chain reaction (RT-qPCR)

Total RNA was extracted from transfected cells using the RNA-Quick Purification Kit (ES Science). Reverse transcription was performed by synthesizing cDNA templates with 5× PrimeScript RT Master Mix (Takara). RT-qPCR was conducted using a 10 μL mixture containing 5 μL Hieff qPCR SYBR Green Master Mix (Yeasen), 3 μL nuclease-free water, 0.5 μL of both forward and reverse primers (**Table 2**), and 1 μL cDNA for target amplification. An internal reference, the 18s-rRNA-hu-R from Sangon Biotech (Shanghai) Co., Ltd., was utilized to standardize mRNA expression levels in cells where LARP1 was knocked down. The 2-ΔΔCT method was utilized to determine the relative levels of expression. PCR reactions were performed with the LightCycler® 480 Instrument II from Roche Diagnostics, all experiments were meticulously replicated three times to ensure the reliability and consistency of the results (n=3).

Cell proliferation assays

Viability of cells was determined by utilizing the Cell Counting Kit-8 (CCK-8; Vazyme Biotech Co., Ltd., Cat A311-02-AA). Following transfection, CAL-62 and KHM-5M cells were placed in

a 96-well plate with 2,000 cells per well and given 8-12 hours to attach. Afterward, CCK-8 reagent was introduced, and the cells were left to incubate for 2 hours in a cell culture incubator. The absorbance at 450 nm was recorded for every well and repeated on a daily basis for five days in a row. In the clonogenic test, cells were seeded at an equivalent concentration in 6-well dishes and incubated at 37°C for a period of 12 days. After fixing the cells with 4% paraformaldehyde, they were stained using 0.1% crystal violet. All experiments were performed in triplicate.

Cell migration and invasion assessments

Cell migration and invasion experiments were carried out with Corning Transwell systems consisting of 24-well plates with a diameter of 6.5 mm and pores measuring 8.0 μm. During the migration experiments, 20,000 cells from the CAL-62 and KHM-5M cell lines were seeded in the top compartment with 200 μL of medium without serum, 48 hours after transfection. The lower chamber was filled with an extra 800 μL of RPMI-1640 medium containing 10% fetal bovine serum. After 24 hours, cells that did not move were removed from the top membrane with a cotton swab, while those that had traveled to the bottom were treated with 4% paraformaldehyde and stained with 0.01% crystal violet for half an hour.

In the invasion assays, 50 μL of Matrigel matrix (Xiamen Mogengel Biotechnology Co., Ltd.) was applied to each well and allowed to polymerize at 37°C for 30 minutes before seeding the cells. Subsequently, 40,000 cells were plated onto the extracellular matrix-coated upper chamber and incubated for 48 hours. Migration and invasion outcomes were captured and analyzed using the EVOS M7000 automated live cell imaging system. All experiments were performed at least three times independently to confirm reproducibility and reliability.

Apoptosis assays

Apoptosis was assessed using the Annexin V-FITC Apoptosis Detection Kit (Multi Sciences Biotech Co., Ltd., Hangzhou, China) following manufacturer instructions. After cell digestion and centrifugation, cells were resuspended in 500 μL of 1× Binding Buffer. Then, 5 μL Annexin V-FITC and 10 μL propidium iodide (PI) were added, followed by a 5-minute incubation at room temperature in the dark. Fluorescence was measured using a NovoCyte Advanteon flow cytometer (Agilent Technologies, Inc.) and analyzed with FlowJo software. This assay distinguishes viable cells (Annexin V-/PI-), early apoptotic cells (Annexin V+/PI-), and late apoptotic/necrotic cells (Annexin V+/PI+).

Cell cycle assays

Cell cycle distribution was analyzed using the Cell Cycle Staining Kit (Multi Sciences Biotech Co., Ltd.) as per the manufacturer's protocol. Transfected cells were collected, stained with 1 mL DNA Staining Solution and 10 μL Permeabilization Solution, and incubated in the dark at room temperature for 30 minutes. Cells were then analyzed by flow cytometry, and data were processed using FlowJo software.

Western blot analysis

After transfection of the CAL-62 and KHM-5M cell lines, the cells were cultured for an additional 48 to 72 hours. Following this incubation period, the cells were harvested and lysed on ice for 10 minutes using a specialized lysis buffer designed for Western blot and immunoprecipitation applications. This lysis buffer included PMSF (#P0013, Beyotime Institute of Biotechnology, China) to inhibit protease activity. Protein concentrations in the lysates were determined using the Bicinchoninic Acid (BCA) Protein Assay Kit (Thermo Fisher Scientific, USA).

Proteins were separated by SDS-PAGE using 4-20% precast Tris-Glycine gels (#P0524M, Beyotime Institute of Biotechnology, China), then transferred onto PVDF membranes. To prevent non-specific binding, membranes were blocked for one hour in TBST containing 1% Tween-20 and 5% non-fat milk. After blocking, membranes were incubated overnight at 4°C with primary antibodies, followed by a 60-minute incubation at room temperature with horseradish peroxidase (HRP)-conjugated secondary antibodies. Proteins were detected with the FDbioDura ECL Kit (#FD8020, Fdbio Science, China) and images were taken using The Cute ChemiDoc Imager (Shenhua Science and Technology Co., Ltd.). Protein band densities were quantitatively analyzed using SHST Analysis software.

Table 3. Distribution of LARP1 expression levels across different clinical samples

	LARP1 expression levels				
	-	1+	2+	3+	4+
Paracancerous Thyroid Tissues (10)	6 (60%)	4 (40%)	0 (0%)	0 (0%)	0 (0%)
PTC (10)	0 (0%)	2 (20%)	5 (50%)	2 (20%)	1 (10%)
ATC (6)	0 (0%)	0 (0%)	0 (0%)	1 (17%)	5 (83%)

Note: The table shows the sample sizes of three different clinical conditions (Paracancerous Thyroid Tissues, PTC, ATC) categorized by LARP1 expression levels, ranging from "-/1+/2+" (low) to "3+/4+" (high) as assessed by immunohistochemistry.

Table 4. Expression level of LARP1 in clinical pathological samples

Variables		PTC (Patients = 10)		ATC (Patients = 6)	
		Low	High	Low	High
		7	3	0	6
Gender	Male	4	0	-	5
	Female	3	3	-	1
Age	< 55	6	3	-	1
	≥ 55	1	0	-	5
Tumor size	< 2 cm	5	2	-	0
	≥ 2 cm	2	1	-	6
Capsule invasion	Yes	6	3	-	6
	No	1	-	-	0
T-status	T1-2	5	2	-	0
	T3-4	2	1	-	6
Lymph node involvement	Yes	7	3	-	5
	No	-	-	-	1
Distant metastasis	Yes	1	-	-	6
	No	6	3	-	0
TNM stage	I-II	7	3	-	0
	III-IV	-	-	-	6

Statistical analysis

GraphPad Prism 9.0 was used for all statistical analyses and data visualization. Differences between two groups were analyzed using the non-parametric Mann-Whitney U test. For comparisons among multiple groups, one-way and two-way ANOVA were performed, followed by Tukey's multiple comparisons post hoc test to identify specific group differences. Repeated Measures ANOVA was employed to analyze cell viability data across multiple time points (0, 24, 48, 72, and 96 hours). Data are presented as mean ± standard deviation, with $P < 0.05$ considered statistically significant. Significance levels are denoted as $*P < 0.05$, $**P < 0.01$, $***P < 0.001$, and $****P < 0.0001$.

Results

The expression of LARP1 is significantly higher in ATC

ATC is a rare but aggressive malignancy. Proteomic analysis of clinical samples revealed that LARP1 is significantly overexpressed in ATC tissues (n = 6) compared to PTC tissues (n = 6) (**Figure 1A**). The non-parametric Mann-Whitney U test was used to compare the mean expression levels of LARP1 between the two groups, yielding a *P*-value that indicated statistical significance ($**P < 0.01$). Immunohistochemical staining further validated the upregulation of LARP1 in ATC cells relative to peritumoral thyroid tissues and PTC (**Figure 1B**). We examined the expression and clinicopathological features of LARP1 in 10 paracancerous thyroid tissues, 10 PTC tissues, and 6 ATC tissues. In our results, 70% of PTC samples showed low expression, with only 30% showing high expression. In contrast, LARP1 was highly expressed in all 6 ATC samples (100%) (**Table 3**). The middle age of the ATC patients was 70 years, with an age range of 54-85 years. Each of the 6 ATC cases presented with primary tumors larger than 2 cm, with all cases showing capsule and tissue invasion, lung metastases, and 5 cases exhibiting concurrent cervical lymph node metastasis (**Table 4**). Western blot analysis was utilized to quantify LARP1 protein expression across normal thyroid cells, PTC and ATC cell lines, revealing a marked elevation of LARP1 protein levels within ATC cell lines (CAL-62, KHM-5M, 8505C, C643, BHT101) compared to PTC cell lines (IHH4, TPC-1) (**Figure 1C**).

LARP1 knockdown significantly inhibits proliferation and colony formation of ATC cells

We investigated the role of LARP1 in ATC using the CAL-62 and KHM-5M cell lines, which initially exhibited high LARP1 expression. To explore LARP1's function, we conducted RNA interference (RNAi) experiments to knock down LARP1 expression, followed by assessments of RNA and protein levels via RT-qPCR and Western blot (WB), respectively. The RT-qPCR results demonstrated a significant decrease in LARP1 mRNA levels in CAL-62 and KHM-5M cells post-RNAi treatment, confirming successful gene silencing at the transcriptional level (**Figure 2A**). Western blot analysis further validated these findings by showing a marked reduction in LARP1 protein levels, indicating effective silencing at the protein level (**Figure 2B**).

To evaluate the functional impact of LARP1 knockdown, we performed CCK8 proliferation assays and colony formation assays. The CCK8 assays revealed a notable reduction in cell growth in the LARP1 knockdown group compared to the control group across multiple time points (0 h, 24 h, 48 h, 72 h, and 96 h) (**Figure 2C**). Integrating the data presented in **Figure 2A-C**, it is evident that although the three siRNAs achieved comparable knockdown efficiencies of LARP1 mRNA and protein levels, the resulting phenotypic effects varied markedly. Notably, LARP1 knockdown in CAL-62 cells led to significant differences in cell viability despite similar silencing efficacy. This observation underscores the biological complexity of LARP1 and may be explained by several potential mechanisms: (i) synergistic inhibition of survival pathways through off-target effects mediated by seed sequence complementarity; (ii) complete elimination of oncogenic LARP1 isoforms; and (iii) surpassing a critical expression threshold necessary to maintain translational fidelity.

Additionally, the colony formation assays indicated a significant decrease in the colony-forming ability of CAL-62 and KHM-5M cells following LARP1 suppression (**Figure 2D**, **2E**). These findings collectively suggest that LARP1 knockdown substantially inhibits the proliferation and colony formation of ATC cells, highlighting the critical role of LARP1 in the growth and expansion of these cancer cells.

LARP1 knockdown leads to increased apoptosis in ATC cells

Post-LARP1 knockdown, morphological observations of ATC cells using the EVOS M7000 intelligent imaging system revealed typical apoptotic changes such as cell shrinkage, membrane blebbing, and nuclear fragmentation (**Figure 3A**). Flow cytometry was used to measure these findings, revealing a notable rise in apoptotic cells after LARP1 knockdown in comparison to the control group (**Figure 3B**, **3C**). This increase was statistically significant ($P < 0.0001$), confirming that reduced LARP1 expression contributes to enhanced apoptotic cell death in ATC cells.

Both morphological observations and flow cytometry data strongly support the essential role of LARP1 in regulating the survival of CAL-62 and KHM-5M cells. These findings highlight LARP1 as a promising candidate for therapeutic targeting in ATC.

LARP1 knockdown induces G2/M phase cell cycle arrest in ATC cells

Flow cytometric analysis revealed that knocking down LARP1 in CAL-62 and KHM-5M cells led to significant changes in cell cycle distribution. Specifically, there was a marked accumulation of cells in the G2/M phase compared to controls (**Figure 4A**). Statistical analysis confirmed this G2/M phase arrest was significant ($P < 0.05$), suggesting that diminished LARP1 expression interferes with normal cell cycle progression, causing cells to arrest at the G2/M checkpoint (**Figure 4B**).

This finding indicates that LARP1 is essential for controlling the cell cycle in ATC cells, underscoring its promise as a target for therapy by disrupting cell cycle advancement and hindering the growth of ATC cells.

LARP1 knockdown reduces migration rate and invasive ability of ATC cells

Transwell migration assays were performed on CAL-62 and KHM-5M cell lines to evaluate how reducing LARP1 affects the ability of ATC cells to migrate. Cell migration was observed and quantified using the EVOS M7000 imaging system. The findings showed a notable decrease in the movement speed of CAL-62 and KHM-5M

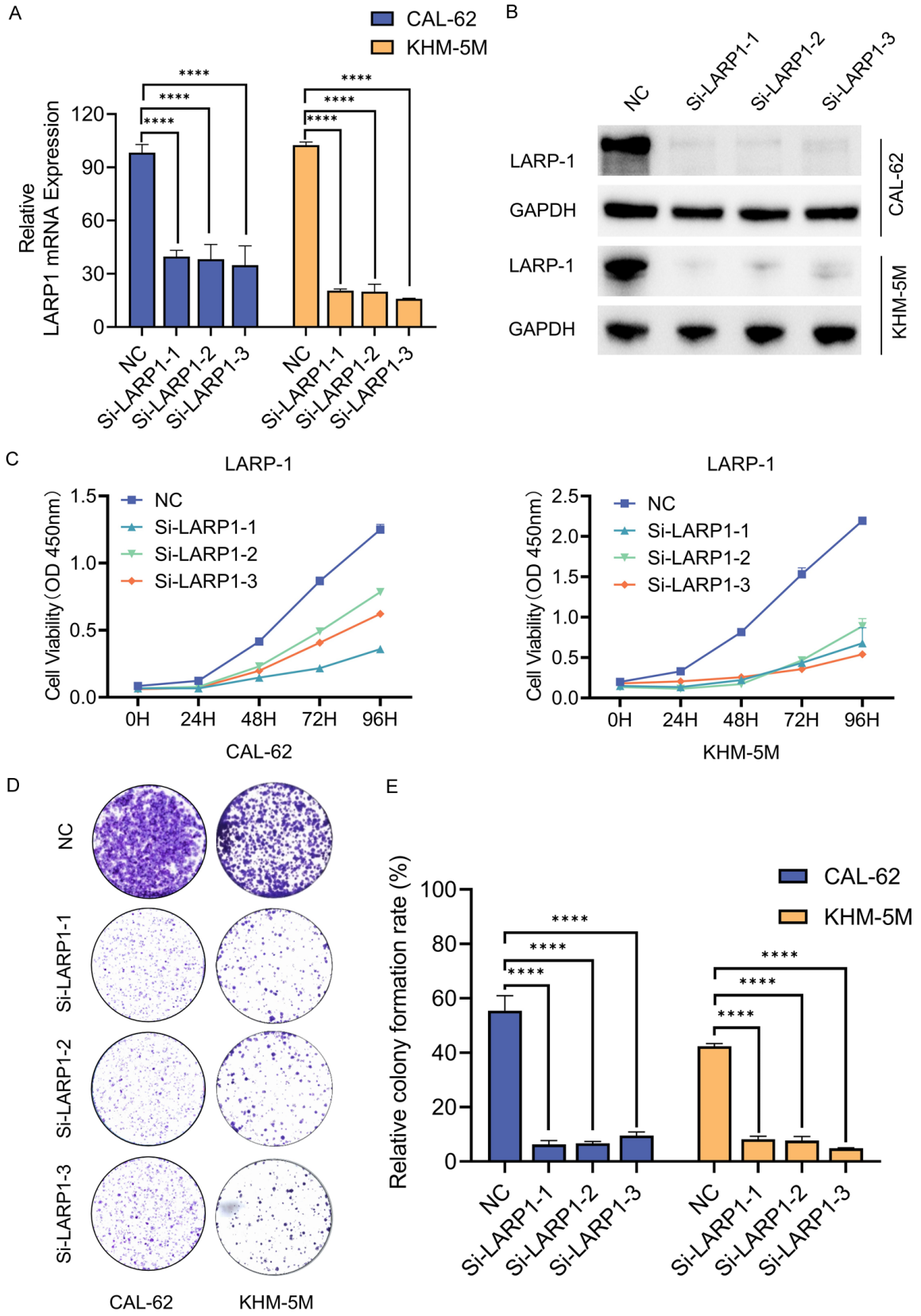

Figure 2. LARP1 expression in CAL-62 and KHM-5M. Knockdown of LARP1 inhibits the proliferation and colony formation of CAL-62 and KHM-5M cells. A. RT-qPCR analysis revealed changes in LARP1 mRNA levels in CAL-62 and

KHM-5M cells upon LARP1 knockdown (mean ± SD) (n = 3 independent replicates each group, **** indicates $P < 0.0001$, compared with control). B. Western blot validation demonstrated a significant decrease in LARP1 protein expression in ATC cells following transfection with LARP1-specific siRNA. C. Downregulating the expression of LARP1 inhibited the proliferation of ATC cells by CCK8 assays (n = 3). D. Inhibition of LARP1 resulted in decreased cell growth in CAL-62 and KHM-5M, as shown by colony formation tests. E. Statistical analysis chart for colony formation experiment (n = 3, **** indicates $P < 0.0001$ compared with control).

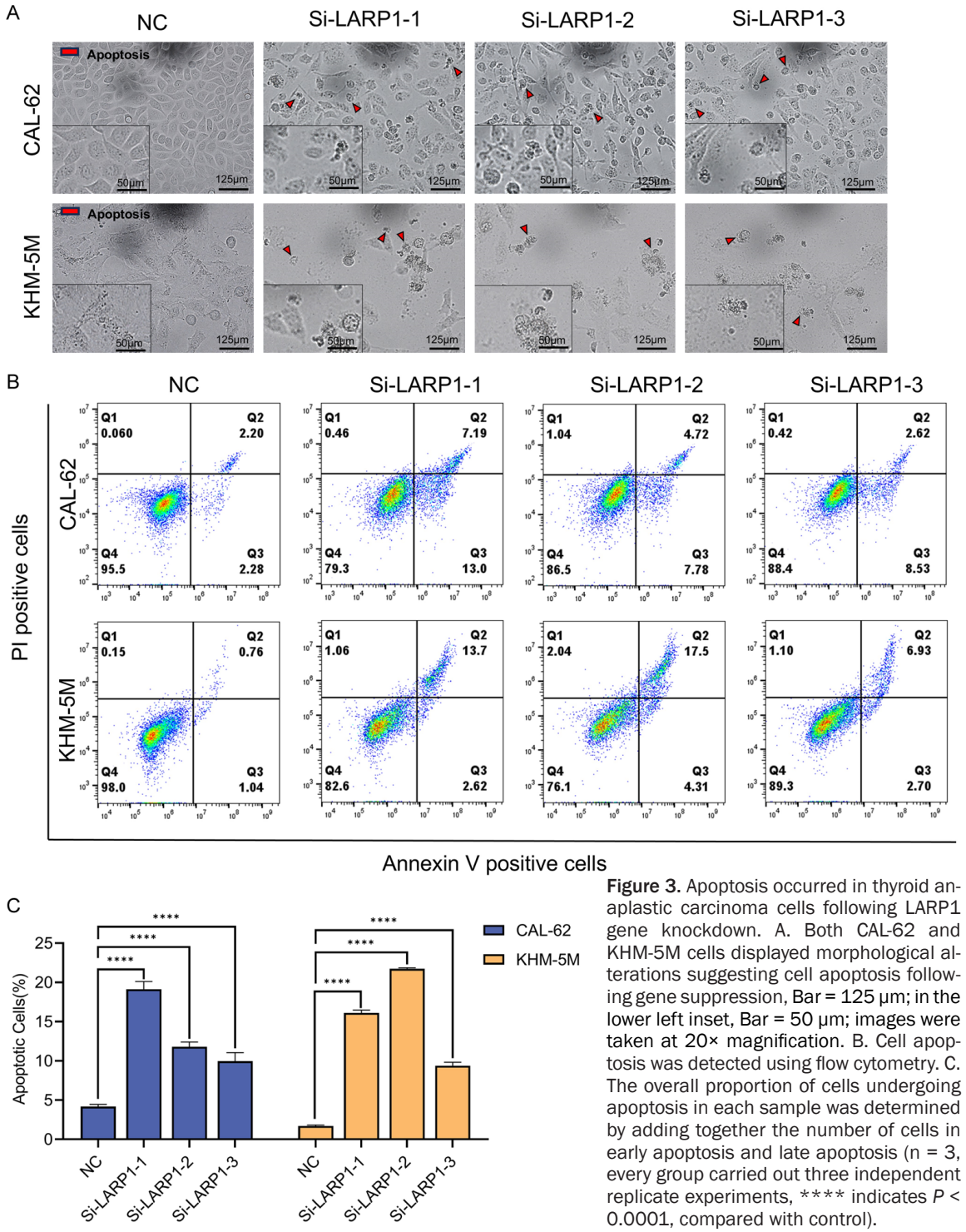

Figure 3. Apoptosis occurred in thyroid anaplastic carcinoma cells following LARP1 gene knockdown. A. Both CAL-62 and KHM-5M cells displayed morphological alterations suggesting cell apoptosis following gene suppression, Bar = 125 μm; in the lower left inset, Bar = 50 μm; images were taken at 20× magnification. B. Cell apoptosis was detected using flow cytometry. C. The overall proportion of cells undergoing apoptosis in each sample was determined by adding together the number of cells in early apoptosis and late apoptosis (n = 3, every group carried out three independent replicate experiments, **** indicates $P < 0.0001$, compared with control).

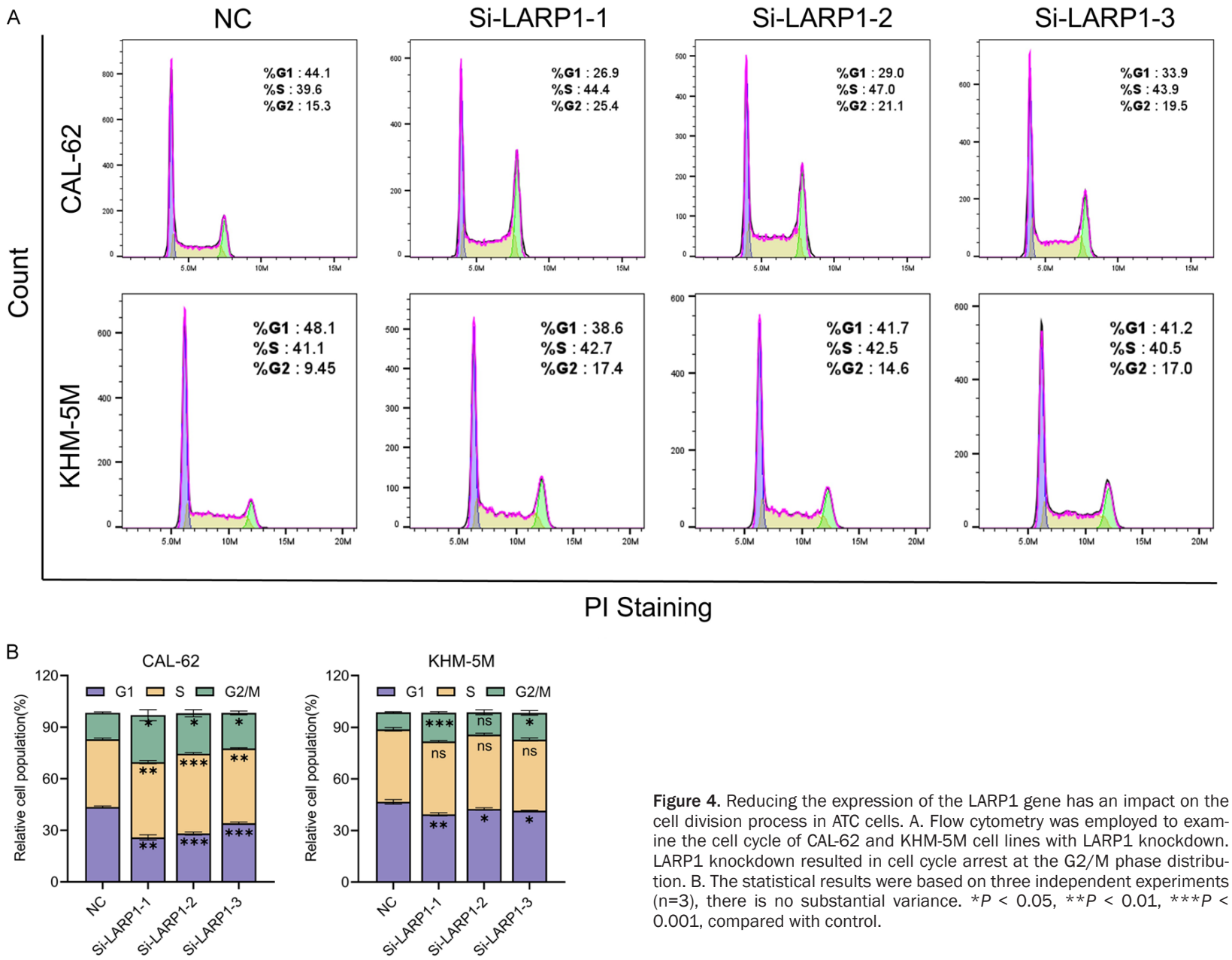

Figure 4. Reducing the expression of the LARP1 gene has an impact on the cell division process in ATC cells. A. Flow cytometry was employed to examine the cell cycle of CAL-62 and KHM-5M cell lines with LARP1 knockdown. LARP1 knockdown resulted in cell cycle arrest at the G2/M phase distribution. B. The statistical results were based on three independent experiments (n=3), there is no substantial variance. *P < 0.05, **P < 0.01, ***P < 0.001, compared with control.

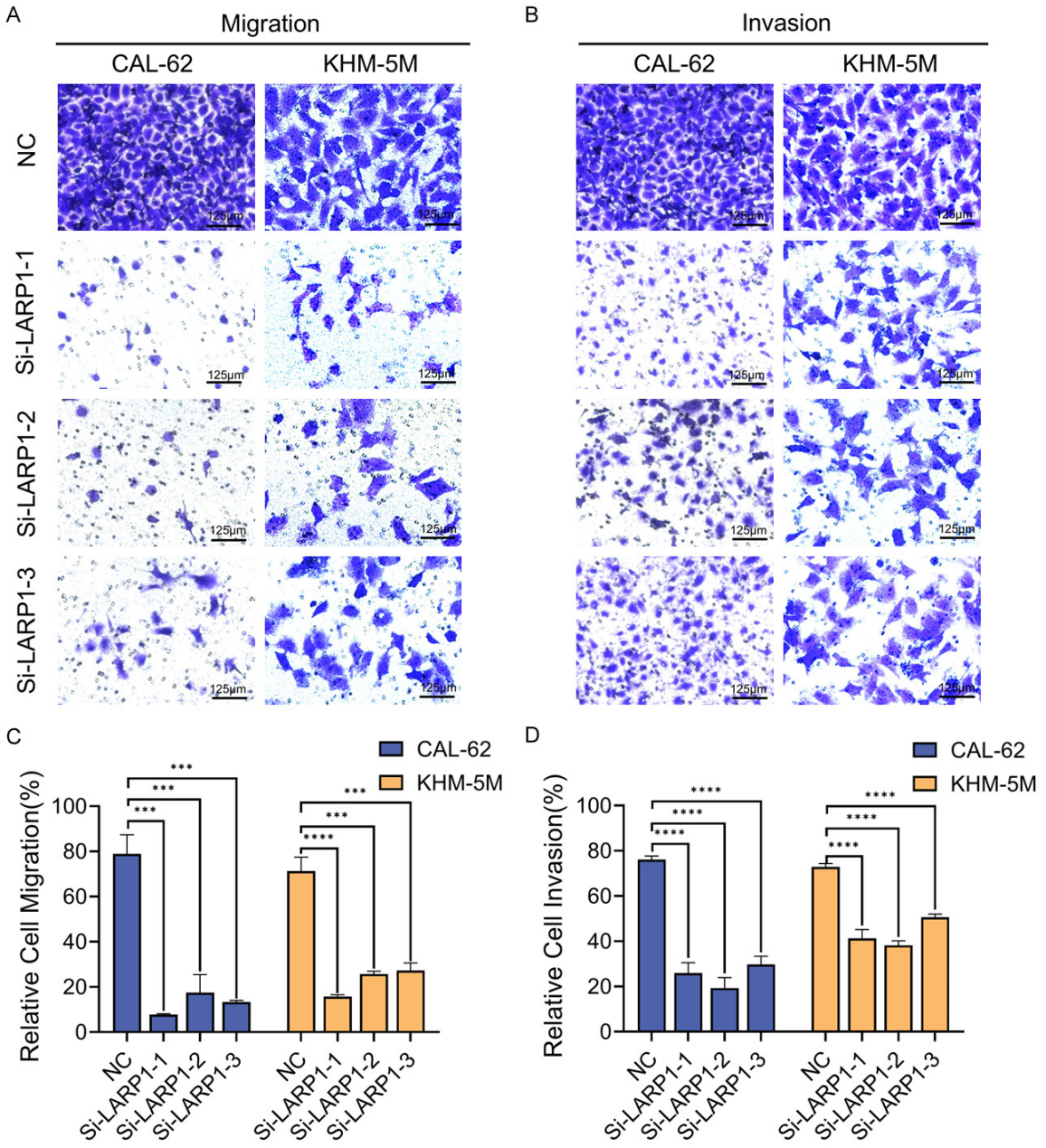

Figure 5. Impact of reducing LARP1 on the migration and invasion of thyroid tumor cells. A, B. Transwell assays showed reduced migration and invasion abilities of CAL-62 and KHM-5M cell lines following LARP1 depletion (transwell assay; crystal violet staining; scale bars, 125 μm; magnification, 20×). C, D. Quantitative statistical graphs of migration and invasion experiments. n=3, each group conducted three independent replicate experiments. *** indicates $P < 0.001$, **** indicates $P < 0.0001$, compared with control.

cells after LARP1 knockdown, in contrast to control cells, suggesting a hindered ability to migrate (**Figure 5A**), the statistical analysis chart for the cell migration experiment is presented in **Figure 5C**. The results indicate that the involvement of LARP1 is essential in the movement of ATC cells.

In the same way, we confirmed the ability of CAL-62 and KHM-5M to invade after reducing LARP1 using Transwell assays. Significant decrease in invasive ability of both cell types observed after LARP1 knockdown, with fewer invading cells in knockdown group compared to controls, suggesting reduced invasiveness

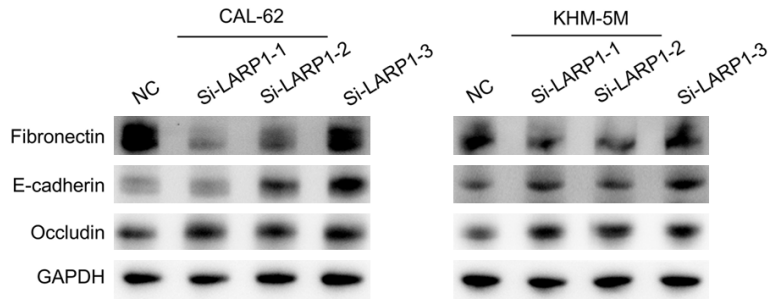

Figure 6. Expression of EMT-related proteins after LARP1 knockdown in KHM-5M and CAL-62 cell lines. Western blot analysis was performed to assess the levels of Fibronectin, E-cadherin and Occludin in all experimental groups.

(**Figure 5B**), the statistical analysis diagram for the cell invasion experiment is shown in **Figure 5D**. These findings underscore LARP1's crucial role in ATC cell invasion, suggesting that its inhibition could reduce the invasiveness and metastatic potential of these cells.

LARP1 knockdown reduces epithelial-mesenchymal transition (EMT) progression of ATC cells

LARP1 knockdown in KHM-5M and CAL-62 ATC cell lines resulted in a notable change in EMT markers, as evidenced by Western blot analysis. In LARP1-depleted cells, the levels of Occludin and E-cadherin, which are epithelial markers, were significantly increased compared to the negative control (NC) group. Conversely, the levels of mesenchymal marker Fibronectin was substantially decreased (**Figure 6**). Fibronectin was selected as the key mesenchymal marker due to its well-established role in ATC metastasis. Previous studies have demonstrated that Fibronectin overexpression is significantly associated with extrathyroidal invasion and distant metastasis in ATC [20]. Additionally, the expression levels of LARP1 and E-cadherin have been shown to correlate closely with tumor TNM stage and lymph node metastasis [21]. Although antibodies against N-cadherin and Vimentin were tested, these markers were ultimately excluded from analysis due to the presence of nonspecific bands in ATC lysates. Western blot assays employing established EMT markers demonstrated that suppression of LARP1 led to decreased Fibronectin levels alongside increased expression of epithelial markers E-cadherin and Occludin. This pattern confirms a reversal of the epithelial-mesenchymal transition process. These results underscore the pivotal role of LARP1 in modulating EMT in ATC cells, potentially influencing their invasive and metastatic capabilities.

Discussion

ATC is one of the most aggressive human malignancies, characterized by rapid onset, extensive local invasion, and frequent distant metastases at diagnosis [22]. Many patients present with unresectable tumors, making ATC one of the most clinically challenging cancers [23]. Due to its aggressive local growth, suffocation often occurs, leading to early mortality in ATC patients [24, 25]. At present, there is no established treatment that notably enhances the survival rates of individuals with ATC [26]. Hence, it is crucial to discover novel molecular indicators and create successful therapeutic approaches for ATC. Our study provides important insights into the role of LARP1 in ATC expression and progression. Through immunohistochemical analysis of 10 PTC samples, paracancerous tissues, and 6 ATC samples, we observed that LARP1 was highly expressed in all ATC tissues, with levels significantly higher than those in PTC tissues. This finding suggests that LARP1 may contribute to the invasive behavior of ATC.

Our study provides novel insights into the role of LARP1 in ATC progression. Immunohistochemical analysis of 10 PTC samples, adjacent tissues, and 6 ATC samples revealed uniformly high LARP1 expression in ATC tissues, significantly exceeding levels observed in PTC. This suggests that LARP1 may contribute to the aggressive invasive phenotype of ATC. Proteomic data corroborated these findings, showing significantly elevated LARP1 protein levels in ATC compared to PTC. Although limited by the rarity of ATC samples (n = 6), clinical pathological analysis confirmed consistent high expression of LARP1 in ATC tumor cells. LARP1 expression was elevated in both PTC and ATC relative to normal thyroid tissue, but markedly higher in ATC, supporting its role in thyroid cancer pathogenesis. ATC is widely recognized as a poorly differentiated and highly aggressive thyroid cancer subtype, in contrast to the generally

less aggressive and well-differentiated PTC [27, 28]. LARP1 has been implicated as an oncogenic factor in other malignancies, where its expression correlates with tumor invasiveness and differentiation status [17]. Our findings suggest that the overexpression of LARP1 in ATC, as contrasted with PTC, aligns with the known association of LARP1 with a more aggressive cancer phenotype.

Functional assays corroborated these observations. Silencing LARP1 in ATC cell lines resulted in significant reductions in proliferation, colony formation, migratory, and invasive capabilities. These results suggest that LARP1 plays a central role in driving the malignant behavior of ATC cells. Additionally, flow cytometric analyses revealed enhanced apoptosis and cell cycle arrest upon LARP1 knockdown, further supporting its oncogenic role in ATC.

The observed G2/M arrest may be explained by impaired translation of 5'TOP mRNAs dependent on LARP1, leading to nucleotide depletion and DNA replication stress, which activates the ATR-Chk1 pathway and disrupts mitotic regulator synthesis [29]. Further detailed mechanistic studies employing CRISPR/Cas9 gene editing are warranted to elucidate this pathway.

This study identified a consistent overexpression of LARP1 in all examined ATC tissues (6/6 cases), distinguishing it markedly from currently established biomarkers in the field of anaplastic thyroid carcinoma. For instance, the BRAF V600E mutation, a well-known oncogenic driver in thyroid cancer, is detected in approximately 25% of ATC cases, with its prognostic value varying considerably due to tumor heterogeneity [30]. In 2018, the U.S. Food and Drug Administration (FDA) approved the combined use of dabrafenib and trametinib for the treatment of locally advanced, unresectable, or metastatic ATC harboring the BRAFV600E mutation; however, clinical outcomes have remained suboptimal [31, 32].

Similarly, although PD-L1 expression correlates with response to immunotherapy, its positivity rate in ATC is approximately 30%, and evaluation of anti-PD-1 antibody efficacy in patients with locally advanced and/or metastatic ATC revealed an overall response rate of 19%, observed exclusively in patients with PD-L1-positive tumors [33]. In contrast, the universal high expression of LARP1 in our cohort (100%) combined with its dual regulatory roles in epithelial-mesenchymal transition (via suppression of Fibronectin) and cell proliferation (through induction of G2/M phase arrest) position it as a more robust and functionally integrative biomarker for ATC.

Western blot analysis demonstrated that LARP1 knockdown markedly downregulated the mesenchymal marker Fibronectin while upregulating the epithelial markers E-cadherin and Occludin (**Figure 6**), indicating a critical regulatory role of LARP1 in the epithelial-mesenchymal transition process. Previous studies in ovarian cancer have shown that LARP1 promotes EMT by binding to and stabilizing Snail mRNA [34]. In ATC, LARP1 may exert similar effects on EMT-related transcripts. Furthermore, the interaction between LARP1 and the mTOR signaling pathway-an established regulator of EMT [17]-may synergistically enhance downstream pro-invasive signaling. Although this study did not directly validate these interactions, the observed reversal of EMT markers strongly implicates LARP1's mechanistic involvement. Future investigations will focus on elucidating LARP1's RNA targets and its cross-regulatory roles within signaling pathways.

These results imply that LARP1 could serve as a valuable molecular marker for ATC. Our findings are consistent with previous studies on the role of LARP1 in cancer progression, although this is the first comprehensive report addressing its role in ATC. The high expression of LARP1 in ATC tissues compared to PTC underscores its potential as a biomarker specific to this aggressive thyroid cancer subtype.

ATC is a highly aggressive and fatal thyroid cancer within the broader category of head and neck tumors, where early diagnosis and intervention are critical [35, 36]. Given the rapid advancements in artificial intelligence (AI) within the field of head and neck tumors, neural networks (NNs), particularly convolutional neural networks (CNNs), could be employed for both macro- and microscopic tumor detection [37]. In future studies, CNNs may be utilized to improve the diagnostic accuracy of immunohistochemical analysis, enabling earlier intervention and more personalized therapeutic strategies by enhancing the detection of LARP1 expression levels in ATC tissues.

Due to the low incidence of ATC and the rapid progression of the tumor, most patients were already in advanced stages and lost the opportunity for surgery by the time of consultation, resulting in a limited window for treatment and survival times of only 3-6 months [25, 38]. Consequently, the number of samples available for analysis was very limited. Although our hospital admitted more ATC patients than most other hospitals, the sample size was still insufficient for robust statistical analysis. The statistical approach in this study was specifically tailored to address the rarity of ATC. Non-parametric tests (Mann-Whitney U test) were employed to minimize assumptions regarding the distribution of the small sample size (n = 6 ATC tissues). However, it is important to acknowledge that the limited sample size may reduce the statistical power to detect subtle effect sizes, increasing the risk of type II errors, and may constrain the generalizability of the findings to the broader ATC population. Therefore, these results should be interpreted with caution until validated in larger cohorts. Future investigations involving multicenter studies with standardized sampling protocols are warranted to confirm the diagnostic universality of LARP1.

Our study emphasizes the critical role of LARP1 in ATC progression and suggests that LARP1 may be a promising therapeutic target. Future research should focus not only on conducting more in-depth mechanistic and in vivo studies to validate the potential of targeting LARP1 in ATC therapy but also on leveraging AI technologies to advance these investigations.

Acknowledgements

We acknowledge this research was supported by the Natural Science Foundation of Zhejiang Province (LQ22H160063); the Zhejiang Medical and Health Science and Technology Project (2022KY064); the Project of Administration of Traditional Chinese Medicine of Zhejiang Province of China (2021ZQ011); the Basic Scientific Research Funds of the Department of Education of Zhejiang Province (KYQN202111); the Outstanding Research Start-up Fund of the People's Hospital of Zhejiang Province (ZRY2020B002); and Administration of Traditional Chinese Medicine of Zhejiang Province, Traditional Chinese Medicine Inheritance and Innovation Talent Support Plan (2023ZR068).

Disclosure of conflict of interest

None.

Address correspondence to: Dr. Chuanming Zheng, Otolaryngology, Head and Neck Center, Cancer Center, Department of Head and Neck Surgery, Zhejiang Provincial People's Hospital (Affiliated People's Hospital), Hangzhou Medical College, No. 158 Shangtang Road, Gongshu District, Hangzhou 310014, Zhejiang, P. R. China. Tel: +86-0571-85893568; E-mail: mingdoc@163.com; Dr. Qingliang Wen, Zhejiang Cancer Hospital, Hangzhou Institute of Medicine (HIM), Chinese Academy of Sciences, No. 1, East Banshan Road, Gongshu District, Hangzhou 310022, Zhejiang, P. R. China. Tel: +86-0571-88122222; E-mail: wenqingliang91@163.com

References

[1] Smallridge RC, Ain KB, Asa SL, Bible KC, Brierley JD, Burman KD, Kebebew E, Lee NY, Nikiforov YE, Rosenthal MS, Shah MH, Shaha AR and Tuttle RM; American Thyroid Association Anaplastic Thyroid Cancer Guidelines Taskforce. American thyroid association guidelines for management of patients with anaplastic thyroid cancer. Thyroid 2012; 22: 1104-1139.

[2] Tang J, Luo Y and Xiao L. USP26 promotes anaplastic thyroid cancer progression by stabilizing TAZ. Cell Death Dis 2022; 13: 326.

[3] Pan Z, Lu X, Xu T, Chen J, Bao L, Li Y, Gong Y, Che Y, Zou X, Tan Z, Huang P and Ge M. Epigenetic inhibition of CTCF by HN1 promotes dedifferentiation and stemness of anaplastic thyroid cancer. Cancer Lett 2024; 580: 216496.

[4] Maniakas A, Dadu R, Busaidy NL, Wang JR, Ferrarotto R, Lu C, Williams MD, Gunn GB, Hofmann MC, Cote G, Sperling J, Gross ND, Sturgis EM, Goepfert RP, Lai SY, Cabanillas ME and Zafereo M. Evaluation of overall survival in patients with anaplastic thyroid carcinoma, 2000-2019. JAMA Oncol 2020; 6: 1397-1404.

[5] Rao SN and Smallridge RC. Anaplastic thyroid cancer: an update. Best Pract Res Clin Endocrinol Metab 2023; 37: 101678.

[6] Perrier ND, Brierley JD and Tuttle RM. Differentiated and anaplastic thyroid carcinoma: major changes in the American joint committee on cancer eighth edition cancer staging manual. CA Cancer J Clin 2018; 68: 55-63.

[7] Iyer PC, Dadu R, Ferrarotto R, Busaidy NL, Habra MA, Zafereo M, Gross N, Hess KR, Gule-Monroe M, Williams MD and Cabanillas ME. Real-world experience with targeted therapy for the treatment of anaplastic thyroid carcinoma. Thyroid 2018; 28: 79-87.

[8] Fagin JA and Wells SA Jr. Biologic and clinical perspectives on thyroid cancer. N Engl J Med 2016; 375: 1054-1067.
[9] Filetti S, Durante C, Hartl D, Leboulleux S, Locati LD, Newbold K, Papotti MG and Berruti A; ESMO Guidelines Committee. Electronic address: clinicalguidelines@esmo.org. Thyroid cancer: ESMO clinical practice guidelines for diagnosis, treatment and follow-up. Ann Oncol 2019; 30: 1856-1883.
[10] Pan Z, Xu T, Bao L, Hu X, Jin T, Chen J, Chen J, Qian Y, Lu X, li L, Zheng G, Zhang Y, Zou X, Song F, Zheng C, Jiang L, Wang J, Tan Z, Huang P and Ge M. CREB3L1 promotes tumor growth and metastasis of anaplastic thyroid carcinoma by remodeling the tumor microenvironment. Mol Cancer 2022; 21: 190.
[11] Gebauer F, Schwarzl T, Valcárcel J and Hentze MW. RNA-binding proteins in human genetic disease. Nat Rev Genet 2021; 22: 185-198.
[12] Hentze MW, Castello A, Schwarzl T and Preiss T. A brave new world of RNA-binding proteins. Nat Rev Mol Cell Biol 2018; 19: 327-341.
[13] Hopkins TG, Mura M, Al-Ashtal HA, Lahr RM, Abd-Latip N, Sweeney K, Lu H, Weir J, El-Bahrawy M, Steel JH, Ghaem-Maghami S, Aboagye EO, Berman AJ and Blagden SP. The RNA-binding protein LARP1 is a post-transcriptional regulator of survival and tumorigenesis in ovarian cancer. Nucleic Acids Res 2016; 44: 1227-1246.
[14] Stavraka C and Blagden S. The la-related proteins, a family with connections to cancer. Biomolecules 2015; 5: 2701-2722.
[15] Gentilella A, Morón-Duran FD, Fuentes P, Zweig-Rocha G, Riaño-Canalias F, Pelletier J, Ruiz M, Turón G, Castaño J, Tauler A, Bueno C, Menéndez P, Kozma SC and Thomas G. Autogenous control of 5'TOP mRNA stability by 40S ribosomes. Mol Cell 2017; 67: 55-70, e4.
[16] Xu Z, Xu J, Lu H, Lin B, Cai S, Guo J, Zang F and Chen R. LARP1 is regulated by the XIST/miR-374a axis and functions as an oncogene in non-small cell lung carcinoma. Oncol Rep 2017; 38: 3659-3667.
[17] Mura M, Hopkins TG, Michael T, Abd-Latip N, Weir J, Aboagye E, Mauri F, Jameson C, Sturge J, Gabra H, Bushell M, Willis AE, Curry E and Blagden SP. LARP1 post-transcriptionally regulates mTOR and contributes to cancer progression. Oncogene 2015; 34: 5025-5036.
[18] Xie C, Huang L, Xie S, Xie D, Zhang G, Wang P, Peng L and Gao Z. LARP1 predict the prognosis for early-stage and AFP-normal hepatocellular carcinoma. J Transl Med 2013; 11: 272.
[19] Ye L, Lin ST, Mi YS, Liu Y, Ma Y, Sun HM, Peng ZH and Fan JW. Overexpression of LARP1 predicts poor prognosis of colorectal cancer and is expected to be a potential therapeutic target. Tumor Biol 2016; 37: 14585-14594.
[20] Wang P, Shang J, Zhao J, Wang K, Guo L, Gu J and Wang W. SRY-related HMG box-2 role in anaplastic thyroid cancer aggressiveness is related to the fibronectin 1 and PI3K/AKT pathway. Mol Med Rep 2020; 21: 1201-1207.
[21] Jiang F, Fang DB, Lin J, Chen Q, Zhu LX and Yu HZ. Correlation of LARP1 and E-cadherin expression with prognosis of intrahepatic cholangiocarcinoma. Int J Clin Exp Pathol 2018; 11: 3559-3566.
[22] Maniakas A, Zafereo M and Cabanillas ME. Anaplastic thyroid cancer. Endocrinol Metab Clin North Am 2022; 51: 391-401.
[23] Sugarman AJ, Huynh LD, Shabro A and Di Cristofano A. Anaplastic thyroid cancer cells upregulate mitochondrial one-carbon metabolism to meet purine demand, eliciting a critical targetable vulnerability. Cancer Lett 2023; 568: 216304.
[24] Brignardello E, Palestini N, Felicetti F, Castiglione A, Piovesan A, Gallo M, Freddi M, Ricardi U, Gasparri G, Ciccone G, Arvat E and Boccuzzi G. Early surgery and survival of patients with anaplastic thyroid carcinoma: analysis of a case series referred to a single institution between 1999 and 2012. Thyroid 2014; 24: 1600-1606.
[25] Wu SS, Lamarre ED, Yalamanchali A, Brauer PR, Hong H, Reddy CA, Yilmaz E, Woody N, Ku JA, Prendes B, Burkey B, Nasr C, Skugor M, Heiden K, Chute DJ, Knauf JA, Campbell SR, Koyfman SA, Geiger JL and Scharpf J. Association of treatment strategies and tumor characteristics with overall survival among patients with anaplastic thyroid cancer: a single-institution 21-year experience. JAMA Otolaryngol Neck Surg 2023; 149: 300-309.
[26] Zhang Y, Xing Z, Liu T, Tang M, Mi L, Zhu J, Wu W and Wei T. Targeted therapy and drug resistance in thyroid cancer. Eur J Med Chem 2022; 238: 114500.
[27] Foote RL, Molina JR, Kasperbauer JL, Lloyd RV, McIver B, Morris JC, Grant CS, Thompson GB, Richards ML, Hay ID, Smallridge RC and Bible KC. Enhanced survival in locoregionally confined anaplastic thyroid carcinoma: a single-institution experience using aggressive multimodal therapy. Thyroid 2011; 21: 25-30.
[28] Stevens A, Meier J, Bhat A, Knight SJ, Vanness DJ and Balentine C. Reassessing surgical guidelines for papillary thyroid cancer impact on survival: expanding indications for lobectomy. Surgery 2023; 174: 542-548.
[29] Haneke K, Schott J, Lindner D, Hollensen AK, Damgaard CK, Mongis C, Knop M, Palm W, Ruggieri A and Stoecklin G. CDK1 couples pro-

liferation with protein synthesis. J Cell Biol 2020; 219: e201906147.
[30] Fallahi P, Ferrari SM, Galdiero MR, Varricchi G, Elia G, Ragusa F, Paparo SR, Benvenga S and Antonelli A. Molecular targets of tyrosine kinase inhibitors in thyroid cancer. Semin Cancer Biol 2022; 79: 180-196.
[31] Lim AM, Taylor GR, Fellowes A, Cameron L, Lee B, Hicks RJ, McArthur GA, Angel C, Solomon B and Rischin D. BRAF inhibition in $BRAF^{V600E}$-positive anaplastic thyroid carcinoma. J Natl Compr Canc Netw 2016; 14: 249-254.
[32] Limberg J, Egan CE, Gray KD, Singh M, Loewenstein Z, Yang Y, Riascos MC, Al Asadi H, Safe P, El Eshaky S, Liang H, Ullmann TM, Wang W, Li W, Zhang T, Xiang J, Stefanova D, Jin MM, Zarnegar R, Fahey TJ and Min IM. Activation of the JAK/STAT pathway leads to BRAF inhibitor resistance in BRAFV600E positive thyroid carcinoma. Mol Cancer Res 2023; 21: 397-410.
[33] Agarwal S, Jung CK, Gaddam P, Hirokawa M, Higashiyama T, Hang JF, Lai WA, Keelawat S, Liu Z, Na HY, Park SY, Fukuoka J, Satoh S, Mussazhanova Z, Nakashima M, Kakudo K and Bychkov A. PD-L1 expression and its modulating factors in anaplastic thyroid carcinoma: a multi-institutional study. Am J Surg Pathol 2024; 48: 1233-1244.
[34] Chen J, Li X, Yang L and Zhang J. Long noncoding RNA LINC01969 promotes ovarian cancer by regulating the miR-144-5p/LARP1 axis as a competing endogenous RNA. Front Cell Dev Biol 2021; 8: 625730.
[35] Shonka DC, Ho A, Chintakuntlawar AV, Geiger JL, Park JC, Seetharamu N, Jasim S, Abdelhamid Ahmed AH, Bible KC, Brose MS, Cabanillas ME, Dabekaussen K, Davies L, Dias-Santagata D, Fagin JA, Faquin WC, Ghossein RA, Gopal RK, Miyauchi A, Nikiforov YE, Ringel MD, Robinson B, Ryder MM, Sherman EJ, Sadow PM, Shin JJ, Stack BC Jr, Tuttle RM, Wirth LJ, Zafereo ME and Randolph GW. American head and neck society endocrine surgery section and international thyroid oncology group consensus statement on mutational testing in thyroid cancer: defining advanced thyroid cancer and its targeted treatment. Head Neck 2022; 44: 1277-1300.
[36] Boucai L, Zafereo M and Cabanillas ME. Thyroid cancer: a review. JAMA 2024; 331: 425-435.
[37] Taciuc IA, Dumitru M, Vrinceanu D, Gherghe M, Manole F, Marinescu A, Serboiu C, Neagos A and Costache A. Applications and challenges of neural networks in otolaryngology (review). Biomed Rep 2024; 20: 92.
[38] Bible KC, Kebebew E, Brierley J, Brito JP, Cabanillas ME, Clark TJ Jr, Di Cristofano A, Foote R, Giordano T, Kasperbauer J, Newbold K, Nikiforov YE, Randolph G, Rosenthal MS, Sawka AM, Shah M, Shaha A, Smallridge R and Wong-Clark CK. 2021 American thyroid association guidelines for management of patients with anaplastic thyroid cancer. Thyroid 2021; 31: 337-386.